THERMAL PERFORMANCE OF A COMPACT SOLAR ASSISTED HEAT PUMP

Samuel Luna Abreu[1], Sérgio Pereira da Rocha[1] and Joaquim Manoel Gonçalves[1]

Instituto Federal de Santa Catarina – Campus São José, São José - SC (Brazil)

1. Introduction

Heat Pumps to supply hot-water for domestic consumption are widely used especially in countries where electric energy is also employed for this purpose. Brazil is a country where most of the domestic hot-water requirements are supplied by electric energy, but basically it is done with electric showers. This solution, although cheap for the user in terms of initial investment, has a strong impact on the generation, transmission and distribution – GTD costs. Electric showers have an average power of more than 5 kW, and are a strong contribution to the residential electric energy end use (around 24% in Brazil (Procel/Eletrobras, 2007)). Also, they are partially responsible by the "peak hour" of the power consumption in the residential sector that occurs from 18:00 to 21:00 hours in Brazil. The consumption growth observed in the last years leads to a lack of reliability of the system, and energy efficiency measures are necessary to avoid risks and to postpone investments in GTD. Solar hot-water systems have been used as an effective way to mitigate the problems caused by the intensive use of electric showers, however, this solution faces some problems when used in low-income housing units: absence of hot-water piping, inadequate structure to install collectors and thermal storage, increase of specific thermal energy costs for small systems, and use of an electric shower as the backup system.

The compact heat pump can be an alternative to electric showers since its use can result in energy savings and reduction in the power demand. The Coefficient Of Performance – *COP* of a heat pump can be more than three times the one of an electric shower and it can be combined with thermal accumulation to reduce the power requirements. The energy for the heat pump can be supplied by photovoltaic panels that can be combined to solar thermal collectors to improve the heat exchange in the cold side of the heat pump.

Rocha et al. (2010) modeled a compact solar assisted heat pump and showed the first obtained results. The present work summarizes aspects of the model simulation showing the outputs of the system as a function of temperature in the hot water tank and solar irradiance.

2. Literature Review

Several authors suggest different configurations of heat pumps assisted by solar energy but the basic assumption of all works is to improve the performance of the equipment using the collected solar thermal energy. In some cases is also considered the possibility of using PV panels to generate the electricity needs for fluid compression.

Kalogirou (2001) proposed a simulation model for a hybrid PV-thermal system where the PV panel acts as the solar collector. Although it does not work integrated with a heat pump, the following conclusions are interesting: (1) the PV-thermal coupling improves the efficiency of the PV panels due to the reduction of the panel temperature; (2) heat and electricity can be produced together. Fraisse et al. (2007) also worked with PV-thermal and highlighted the importance of a good coupling between the PV and thermal collectors suggesting that both should be integrated during the manufacturing process. On the other hand, one of the disadvantages of PV-thermal systems is that as the temperature increases, the PV efficiency drops so the thermal accumulation will decrease the electric performance. The opposite is also true, efficient thermal collectors are not desirable to avoid overheating of the PV panels limiting the thermal performance of the system.

An alternative to surpass this problem is to couple the PV-thermal collector to the evaporator of a heat pump. Heat pumps transfer heat throw a fluid working between a heat source and a heat sink, so the temperature of the evaporator (connected to the heat source) is always lower than the condenser temperature (connected to the heat sink – the thermal storage). In this case, efficient solar thermal collectors are not necessary and the

working fluid evaporation keeps the PV panel in a low temperature increasing its efficiency. This kind of system is usually called "Photovoltaic-Solar Assisted Heat Pump" and will be referred as PV-SAHP.

Pei et al. (2007) developed a PV-SAHP and observed that the performance of the PV panels was improved due to the temperature reduction. Pei et al. (2007) also studied the influence of the solar thermal collectors on the performance of the heat pump. The "Coefficient of Performance" – *COP* is the most known way to evaluate the performance of heat pumps and Equation 1 shows how it can be obtained:

$$COP = \dot{Q}_C / \dot{W}_{comp} \quad \text{(eq. 1)}$$

where $\dot{Q}_C$ is the useful heat on the condenser and $\dot{W}_{comp}$ is the compressor power. Obtained results indicate that the PV-SAHP has a better *COP* and operational conditions can be adjusted varying the compressor frequency.

This work was continued by Ji et al. (2008) where they studied a new PV-SAHP configuration. Using R22 as the working fluid and a compressor power between 150 and 1300 W they analyze the behavior of the condenser capacity, compressor power, PV generated power and *COP* along the day. It was observed that the maximum *COP* and PV power were found during the irradiation peak period around noon. The same result is not verified for the compressor power since it presents a slightly decrease as the solar irradiation increases and the opposite when the solar irradiation decreases. Ji et al. (2009) completed this work presenting a mathematical model to calculate the temperatures and efficiencies of the main components. The authors considered that the model shows a good agreement since the errors on the thermal performance were under 10%.

In the present work, a theoretical study is conducted for a mini heat pump with R134A as the working fluid that is coupled to a solar thermal collector and a PV panel. The system was designed to attend the hot water necessities only for bath purposes for one single person or a small family. The main objective of the present work is to show a sensibility analysis of the theoretical model regarding some design parameters and also to have an idea about the working characteristics of this equipment before the prototype construction.

3. Simulation Model

Figure 1 shows a schematic diagram of the mini heat pump integrated with the PV panel and the solar collector. This is a complete version of the proposed development, but some possibilities are not explored in the present paper and should be better evaluated in the future. The main idea is to have a validate model for a simpler configuration and, as the work evolves, new improvements can be added without doing relevant modifications in the model.

It can be observed that both the PV panel and the solar collector receive solar irradiation that is transformed in electric or thermal energy respectively. The generated electricity is used to supply energy for the electric components of the system: compressor, recirculation pump and actuators. The equipments can work using AC or DC power, so the Power Controller box should be selected in order to attend the chosen configuration, having the capability to transform DC to AC and providing electricity from the grid when necessary.

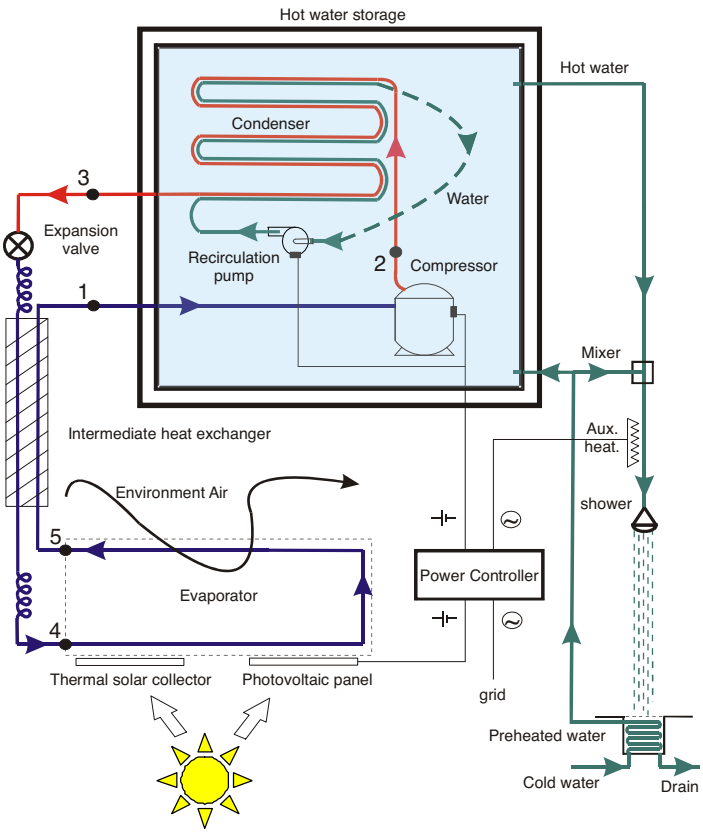

Fig. 1: Schematic diagram of the proposed PV-solar assisted heat pump

The heat absorbed in the solar collector is used to evaporate the working fluid in the cold side of the heat pump improving the *COP* of the heat pump. The recirculation pump has the function of make benefit of the thermal stratification of the hot water tank to improve the heat exchange on the condenser. The recirculation pump, compressor and condenser were installed inside the hot water tank, so all the rejected heat is used to heat water. In the case of using not waterproof equipments, the compressor and pump can be removed from the thermal storage. The use of this complete configuration implies in a complex conception of the hot water tank so the detailed study of the influence of this components in the global performance of the system should be done later as a further development.

The hot water consumption occurs through a thermostatic mixing valve that receives water from the thermal storage and the water mains. Additional heating, can be done by an adjustable electric heater located just after the mixing valve. Although this capability is not included in the model yet, the water from the mains can be pre-heated by the grey water using a heat exchanger located inside the drain, recovering part of the heat usually lost.

The basis of the heat pump model is the work of Gonçalves et al. (2009) that presented a semi-empiric model for steady-state simulation of frost-free domestic refrigerators. This model divides the system in modules where each component is represented by its characteristics equations, whose input and output data creates interdependence among the components. Choosing the correct set of equations it is possible to solve the complete system finding its working characteristics that can be used for design purposes.

Basically these equations represent the heat transfer phenomena on the components and the changes on the thermodynamics properties in the working fluid between the input and output, so the output from a component is used as the input for the following component. Figure 2 shows the thermodynamic cycle of the working fluid on a p x h diagram. The numbered points represent the transition between adjacent components.

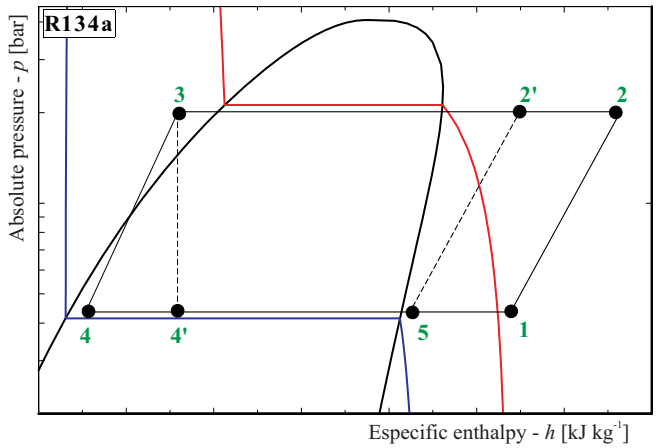

Fig. 2: Pressure versus enthalpy Schematic diagram of the proposed PV-solar assisted heat pump

The process 1-2 represents the isentropic compression of the working fluid where the work is added to the system and heat is rejected inside the hot water tank. During the condensation process 2-3, first sensible cooling is observed, then the condensation itself occurs and finally the subcooling guarantees that only fluid in the liquid phase enters the expansion valve where the pressure of the working fluid drops from the high to the low pressure (process 3-4). The evaporation process 4-5 is improved by the heat collected by the PV and thermal solar collectors. To guarantee that only fluid on the gaseous phase arrives the compressor, an intermediary heat exchanger overheats the fluid in the process 5-1. This also avoids that too much fluid evaporates during the expansion improving the thermal performance of the evaporator.

In the next items, the components used in the simulation model are detailed.

3.1. Model input data

Some parameters during the simulation process are assumed to be fixed and are showed in Table 1.

Tab. 1: Model input data

Name	Symbol [unit]	Valor	Nome	Símbolo [Unidade]	Valor
superheating	ΔT_{sup} [K]	1,0	**compressor overall thermal conductance**	UA_{comp} [WK^{-1}]	1,0
subcooling	ΔT_{sub} [K]	1,0	**condenser overall thermal conductance**	UA_C [WK^{-1}]	100,0
water specific heat	$c_{p,water}$ [J (kgK)$^{-1}$]	4,186	**compressor volumetric displacement**	V_{comp} [cm^3]	1,4
water pressure drop	Δp_{water} [kPa]	50	**photovoltaic efficiency**	η_{PV} [-]	0,1
water specific volume	υ_{water} [m^{3}kg^{-1}]	0,001	**recirculation pump efficiency**	η_{pump} [-]	0,3
water mass flow	$\dot{m}_{water}$ [kg s^{-1}]	0,02	**solar thermal collector area**	A_{col} [m^2]	0,2
efetiveness of the intermediary heat exchanger	ε_{IHE} [-]	0,0	**PV panel area**	A_{PV} [m^2]	1,0

3.2. Compressor

The objective of the compressor analysis is to determine parameters like fluid mass flow displaced by the compressor, power consumption and output thermodynamic properties of the working fluid. As a first approach, the present work uses data available in the manufacturer technical sheet of a commercial compressor that can be observed in Table 2. The compressor size is compared with a coin in the right side of Table 2 giving an idea of its small dimension.

Tab. 2: Picture and technical data of the compressor (Aspen, 2009)

	Condensation temperature - T_C [°C]	26,7 a 71,1
	Evaporation temperature - T_E [°C]	-1,1 a 21,1
	Coefficient of performance - *COP* [-]	0,4 a 9,6
	Cooling capacity – *CC* [W]	58 a 613
	rotation - *N* [rpm]	3000 a 6000

According Gosney (1982), the volumetric and global efficiencies of the compressor, η_v and η_g, can be determined as a function of working characteristics of the compressor: condensation and evaporation temperatures (T_C and T_E), rotation (N) and compression ratio (CR). The compression ratio is given as the ratio between the condensation and evaporation pressures, so $CR = p_C / p_E$. Using performance data provided in the technical sheet from the supplier equations 2 and 3 can be derived. The values of the adjusted coefficients are given in Table 3.

$$\eta_v = a_1 + a_2 T_C + a_3 T_E + a_4 N + a_5 RC + a_6 T_C T_E + a_7 T_C N + a_8 T_C RC + a_9 T_E N + a_{10} T_E RC + a_{11} N RC \quad \text{(eq. 2)}$$

$$\eta_g = b_1 + b_2 T_C + b_3 T_E + b_4 N + b_5 RC + b_6 T_C T_E + b_7 T_C N + b_8 T_C RC + b_9 T_E N + b_{10} T_E RC + b_{11} N RC \quad \text{(eq. 3)}$$

Tab. 3: Coefficients a_n and b_n adjusted for equations 2 and 3.

$\mathbf{a_1}$	9.6375×10^{-1}	$\mathbf{a_7}$	5.9617×10^{-8}	$\mathbf{b_1}$	1.2534×10^{0}	$\mathbf{b_7}$	2.3953×10^{-6}
$\mathbf{a_2}$	7.5308×10^{-3}	$\mathbf{a_8}$	1.7961×10^{-4}	$\mathbf{b_2}$	7.5697×10^{-2}	$\mathbf{b_8}$	8.2607×10^{-3}
$\mathbf{a_3}$	5.1875×10^{-3}	$\mathbf{a_9}$	-1.9711×10^{-6}	$\mathbf{b_3}$	-2.5956×10^{-2}	$\mathbf{b_9}$	-3.0970×10^{-6}
$\mathbf{a_4}$	7.1382×10^{-6}	$\mathbf{a_{10}}$	1.2424×10^{-3}	$\mathbf{b_4}$	-5.1088×10^{-6}	$\mathbf{b_{10}}$	-2.3759×10^{-2}
$\mathbf{a_5}$	-1.6677×10^{-1}	$\mathbf{a_{11}}$	3.5009×10^{-6}	$\mathbf{b_5}$	-1.4662×10^{0}	$\mathbf{b_{11}}$	-2.0941×10^{-5}
$\mathbf{a_6}$	-2.2132×10^{-4}			$\mathbf{b_6}$	-5.8892×10^{-4}		

To determine the mass flow of the working fluid in the heat pump circuit, $\dot{m}_{HP}$ (kg s^{-1}), it is necessary to know the volumetric efficiency given by equation 2 (dimensionless); compressor rotation (Hz); specific volume of the working fluid in the compressor inlet (point 1) (m^{3}kg^{-1}); and displacement volume of the compressor (m^3).

$$\dot{m}_{HP} = \frac{\eta_v V_{comp} N}{v_1} \quad \text{(eq. 4)}$$

The compressor power, $\dot{W}_{comp}$ (W), is calculated using equation 5, where h_{2s} is the isentropic enthalpy in the output of the compressor and h_1 the enthalpy value in the input (J kg^{-1}). The values of the mass flow and global efficiency are given by equations 4 and 3 respectively.

$$\dot{W}_{comp} = \frac{\dot{m}_{HP}(h_{2s} - h_1)}{\eta_g} \quad \text{(eq. 5)}$$

The heat losses of the compressor, $\dot{Q}_{comp}$ (W), are determined by equation 6 considering process 1-2 an adiabatic compression. In this equation $c_{p,2,a}$ and $T_{2,a}$ are respectively the specific heat and temperature of the working fluid in point 2 considering an adiabatic compression.

$$\dot{Q}_{comp} = \dot{m}_{HP} c_{p,2,a} \varepsilon_{comp} (T_{2,a} - T_C) \quad \text{(eq. 6)}$$

The compressor heat transfer effectiveness, ε_{comp} (dimensionless), is given by equation 7:

$$\varepsilon_{comp} = 1 - e^{\left(\frac{-UA_{comp}}{\dot{m}_{HP} c_{p,2,a}}\right)} \quad \text{(eq. 7)}$$

The value of $T_{2,a}$ is calculated from two known thermodynamics properties: the condensation pressure and the adiabatic enthalpy of the working fluid in the output of the compressor determined using equation 8.

$$h_{2,a} = h_1 + \dot{W}_{comp} / \dot{m}_{HP} \quad \text{(eq. 8)}$$

Finally, to determine the temperature at the output of the compressor, T_2, it is necessary to know another thermodynamic property than the condensation pressure. From the energy conservation between the input and output of the compressor it is possible to find the enthalpy at point 2 as shown in equation 9.

$$h_2 = h_1 + (\dot{W}_{comp} - \dot{Q}_{comp}) / \dot{m}_{HP} \quad \text{(eq. 9)}$$

3.3 Condenser and hot water tank

Since the condenser is immersed in the hot water tank, all the heat rejected is transferred to the water, so the heat flow rate from the condensation process 2-3 is the same used for water heating. Equations 10 and 11 are used to calculate the heat flow rate on the working fluid side (10) and hot water side (11).

$$\dot{Q}_C = \dot{m}_{HP}(h_2 - h_3) \quad \text{(eq. 10)}$$

$$\dot{Q}_C = \dot{m}_{water} c_{p,water} \varepsilon_C (T_C - T_{water}) \quad \text{(eq. 11)}$$

where ε_C is the condenser effectiveness (equation 12); $c_{p,water}$ is the water specific heat (J kg^{-1}K^{-1}) and $\dot{m}_{water}$ is the mass flow of the recirculation pump (kg s^{-1}).

$$\varepsilon_C = 1 - e^{\left(\frac{-UA_C}{\dot{m}_{water} c_{p,water}}\right)} \quad \text{(eq. 12)}$$

3.4 Intermediary heat exchanger

One of the ways to improve the *COP* of the heat pump is avoiding the evaporation during the expansion process 3-4. Using an intermediary heat exchanger, it is possible to combine this with the superheating of the fluid (process 5-1) necessary to guarantee that only gas arrives in the compressor. Using the effectiveness of the intermediary heat exchanger (ε_{IHE}), it is possible to determine the input temperature in the compressor as shown in equation 13.

$$T_1 = T_5 + \varepsilon_{IHE}(T_3 - T_5) \quad \text{(eq. 13)}$$

In the present work, ε_{IHE} was set to zero, so the compressor input temperature (T_1) is equal to the output of the evaporator (T_5).

The enthalpy in the output of the expansion valve (h_4) is calculated doing the energy balance for this point. Since the heat rejected in the hot side of the intermediary heat exchanger is the same of the absorbed in the cold side and both mass flows are equal, equation 14 can be used to evaluate h_4.

$$h_4 = h'_4 - (h_1 - h_5) \quad \text{(eq. 14)}$$

Considering an isoenthalpic expansion (figure 2), the enthalpies in the input and output of the expansion valve are the same ($h_3 = h_4'$). As ε_{IHE} was set to zero, in the studied case $h_4 = h_4'$.

3.5 Evaporator, PV panel and solar thermal collector

The heat flow rate in the evaporator $\dot{Q}_E$ is determined by the energy balance on this component as shown in equation 15.

$$\dot{Q}_E = \dot{m}_{HP}(h_1 - h_4) \text{ (eq. 15)}$$

This heat flow can also be considered by the solar thermal collector side using equation 16, where $G_{t,tilt}$ is the global irradiance on the tilted plan where the collector is installed (W.m^{-2}), A_{col} is the solar thermal collector area (m^2) and η_{col} is the solar thermal collector efficiency (dimensionless).

$$\dot{Q}_E = G_{t,tilt} A_{col} \eta_{col} \text{ (eq. 16)}$$

The solar thermal collector efficiency in its linear form is given by equation 17.

$$\eta_{col} = F_R(\tau\alpha) - F_R U_L \frac{T_E - T_a}{G_{t,tilt}} \text{ (eq. 17)}$$

The linear coefficient of the efficiency curve $F_R(\tau\alpha)$ (dimensionless) is a parameter that represents the optical efficiency of the collector and the angular coefficient $F_R U_L$ (Wm^{-2}K^{-1}) represents global heat losses of the collector. Both can be obtained experimentally and will be treated separately from the PV panel in this work. T_E is the evaporator temperature and T_a is the ambient temperature.

Combining equations 16 and 17 it is possible to determinate T_E and consequently the evaporation pressure P_E, that allows the determination of the compression ratio (*CR*) used in equations 2 and 3. The temperature T_1 can be obtained just adding the given superheating (Table 1), so $T_1 = T_E + \Delta T_{\sup}$. With these two thermodynamic properties, other properties in point 1 can also be determined: h_1 in equation 14, v_1 in equation 4 and the entropy s_1. Since the compression process 1-2 is isentropic, $s_1 = s_2$ and together with T_E it is used to determine the properties in point 2.

Table 4 shows two characteristic efficiency curves of solar thermal collectors used in the present work: (i) unglazed collector without insulation and (ii) glazed flat-plate collector with back insulation. These values are only a first reference, since they are based in collectors working with water instead the two-phase flow of the working fluid used in this work.

Tab. 4: Coefficients a_n and b_n adjusted for equations 2 and 3.

Solar collector type	$F_R(\tau\alpha)_e$, [-]	$F_R U_L$, [Wm^{-2}K^{-1}]
glazed flat-plate	0,75	5
unglazed flat-plate	0,95	25

The produced electric power by the PV panel is calculated from its efficiency as shown in equation 18.

$$\dot{W}_{PV} = \eta_{PV} A_{PV} G_{t,tilt} \text{ (eq. 18)}$$

When the solar thermal collector and the PV panel are coupled, it is necessary to consider that part of the available global irradiance will be transformed in electricity. The global irradiance in equations 16 and 17 should consider this effect and can be rewritten changing $G_{t,tilt}$ by $G_{t,tilt}'$ defined by equation 19.

$$G_{t,tilt}' = (1 - \eta_{PV}) G_{t,tilt} \text{ (eq. 19)}$$

Although the coupling between the thermal and PV collectors decreases available solar irradiance for thermal purposes, the efficiency of the PV panel is increased by its temperature reduction. This effect was not analyzed in this work.

3.6 Recirculation pump

The recirculation pump has the objective of improve the heat exchange inside the hot water tank between the condenser and the water, so the water at lower temperature from the bottom of the tank is forced through a heat exchanger constructed around the condenser. The power consumption of the pump $\dot{W}_{pump}$ (W) is calculated using equation 20, where $\dot{m}_w$, Δp_{water} , η_{pump} and v_{water} are given in Table 1.

$$\dot{W}_{pump} = \frac{\dot{m}_{water} \Delta p_{water} v_{water}}{\eta_{pump}} \quad \text{(eq. 20)}$$

In the case that the recirculation pump is not used, the NTU method cannot be implemented as done in item 3.3 and the model for the condenser should be revised.

3.7 Coefficient of Performance - COP

The useful heating rate of the system $\dot{Q}_{heat}$ (W) for water heating in the thermal storage includes the rejected heat in the condenser, water recirculation pump and compressor. The total amount electrical power $\dot{W}_t$ (W) used in the system is given by the sum of compression and pumping powers. From the definition of COP as the ratio between the useful and expended energies, it can be defined for the proposed heat pump by equation 21.

$$COP = \frac{\dot{Q}_{heat}}{\dot{W}_t} = \frac{\dot{Q}_C + \dot{Q}_{comp} + \dot{W}_{pump}}{\dot{W}_{comp} + \dot{W}_{pump}} \quad \text{(eq. 21)}$$

4. Results

The presented results will consider variations in three input parameters: (1) solar irradiance (100 to 1,000 W.m^{-2}); (2) water temperature in the thermal storage (25 to 55 °C); and (3) ambient temperature (10, 20 or 30°C – 20ºC was used as the reference temperature in other cases). All graphics show the behavior of the heat pump for selected operational conditions showing curves for the glazed and unglazed flat-plate solar collectors.

During the simulations it was considered that the thermal collector is coupled to the evaporator, and all electric energy used in the pump and compressor was produced by the PV-panel. Limiting conditions of the system work due to small irradiance level were not taken in consideration in this work.

4.1 Compressor rotation

Figure 3 shows the control map of the compressor rotation for water temperature and solar irradiance variations. The output power of the PV-panel is also showed and it is proportional to the solar radiation since a constant efficiency was used. The compressor rotation is limited by the available electricity so it increases for high solar irradiance levels. It is also observed that as the temperature of the hot water tank increases the rotation decreases as a consequence of the larger difference between the evaporation and condensation pressures. Both curves for the two simulated collectors have similar behaviors.

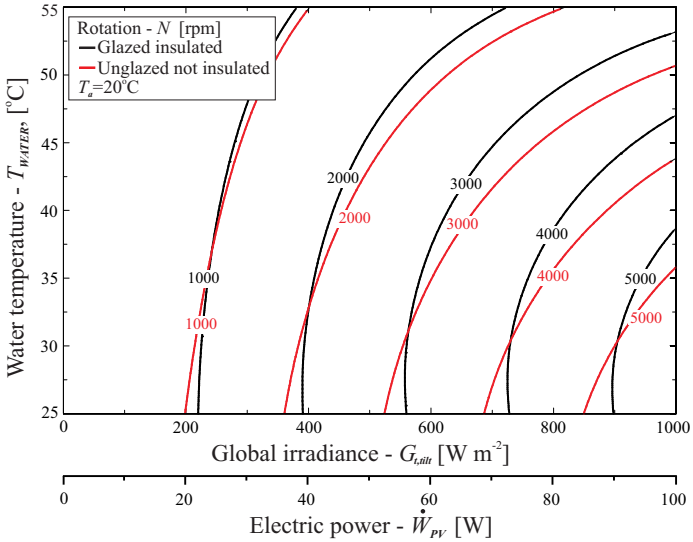

Fig. 3: Control map of the compressor rotation as a function of the water temperature and solar irradiance.

4.2 Condensation and evaporation temperatures

Figures 4a and 4b shows the condensation and evaporation temperatures respectively. It is clearly observed that the condensation temperature is regulated by the temperature of the hot water tank (Figure 4a). For low levels of irradiance, almost no heat is rejected and the condensation and water temperature are almost the same. As the irradiance increases, the difference between these temperatures also increases and consequently the heat transferred to the hot water tank. Figure 4b shows that the evaporation temperature in the glazed collector is lower. Since the compressor power is limited by the available solar irradiance as shown in section 4.1, lower evaporation temperatures implies in higher compressor powers so the heat pump has more difficult to transport heat from the cold to the hot sides. At low levels of irradiance, the evaporation process does not occur and the evaporation temperature tends to the ambient temperature.

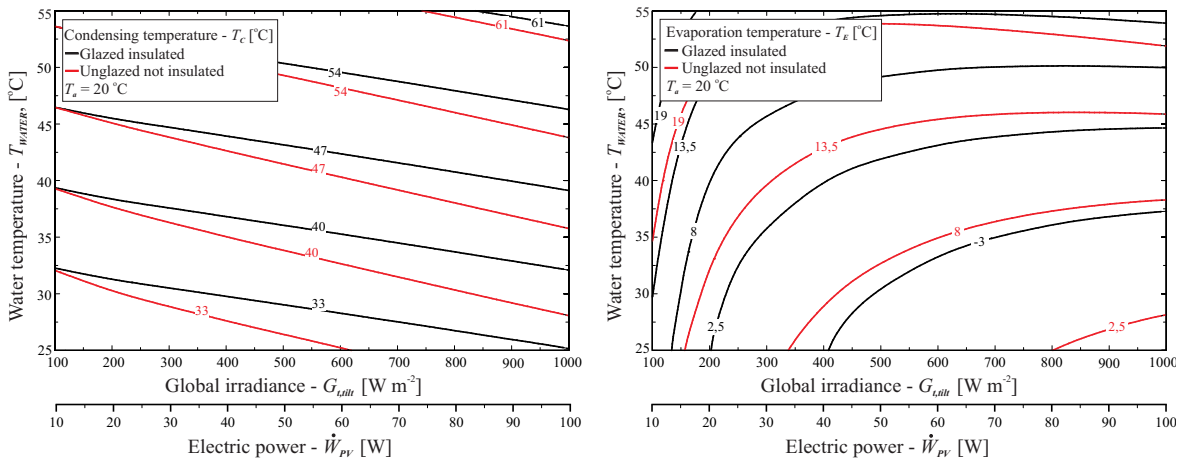

(a) (b)

Fig. 4: Condensation and evaporation temperatures as a function of the water temperature and solar irradiance.

4.3 Heating rate

The heating rate of the system is the most important output of the model. Figure 5a shows its variation for the two chosen solar thermal collectors and it can be observed that the performance of the unglazed collector is better. This is auspicious since the cost of this kind of collector is low and it can be easily construct using industrial processes from refrigeration component manufacturers. Preliminary calculation estimates that the

5. Conclusions

The main objective of the present work that was to develop a model that shows the integration among the heat pump, solar thermal collector and PV-panel was achieved. This can be observed through the variations in the operational conditions induced by the solar irradiation and ambient temperature. The performance of the system is better using cheaper unglazed collectors than glazed back insulated ones, which is very important in terms of cost reduction of the whole system. The proposed configuration can deliver around 50 liters of hot-water per day without necessity of any kind of external energy, which fulfill the requirements for one single person. The same model can be used to size the system for other heating demands just changing the input data.

The possibility to connect the PV-SAHP the grid shown in figure 1 was not taken into account in the present work. Its use implies in additional study to determine the best balance among solar thermal, PV generated electricity and grid supplied electricity that returns the most financially feasible or the best performance configuration.

The next step of the development will be the construction of the first prototype to validate the model. Results from the prototype will be used to refine the critical components of the model. More realistic characterization of the components is also necessary, since in the present model informations like heat transfer coefficients of the heat exchanges (condenser, evaporator, etc.) were only first approaches. After this, configurations for specific applications will be optimized using the same model and real climatic data from solar irradiance and ambient temperature.

6. References

Aspen, 2009. Compressor Aspen, model 14-24-000X technical sheet. (Available in: http://www.aspencompressor.com/products.htm, last accessed on august 10th, 2011).

Fraisse, G., Ménézo, C., Johannes, K., 2007. Energy performance of water hybrid PV/T collectors applied to combisystems of direct solar floor type. J. Solar Energy. 81, 1426-1438.

Gonçalves, J.M., Melo, C., Hermes, C.J.L., 2009. A semi-empirical model for steady-stade simulation of household refrigerators. J.Applied Thermal Engineering. 29, 1622-1630.

Gosney, W. C., 1982. Principles of refrigeration. Cambridge University Press, Cambridge, UK.

Ji J., Pei G., Chow, T. T., Liu K. L., He H., Lu J., Han C., 2008. Experimental study of photovoltaic solar assisted heat pump system. J. Solar Energy. 82, 43-52.

Ji J., He H., Chow, T., Pei G., He W., Liu K., 2009. Distributed dynamic modeling and experimental study of PV evaporator in a PV/T solar-assisted heat pump. I. J. of Heat and Mass Transfer. 52, 1365-1373.

Kalogirou, S. A., 2001. Use of TRNSYS for modelling and simulation of a hybrid PV-thermal solar system for Cyprus. J. Renewable Energy. 23, 247-260.

Pei G., Ji J., Han C., Fan W., 2007. Performance of solar assisted heat pump using PV evaporator under different compressor frequency. Proceedings of ISES Solar World Congress 2007: Solar Energy and Human Settlement. 935-939.

Procel/Eletrobras, 2007. Evaluation of market efficiency in Brazil, research of appliances possession and habits of use, base year 2005, class residential (in Portuguese). 187.

Rocha, S.P., Gonçalves, J.M., Abreu, S.L., 2010, Mini-Heat pump coupled to solar collectors (in Portuguese). III Brazilian Congress on Solar Energy, 21 a 24 de setembro, Belém, Pará, Brasil.